Rational design approach for evaluating fire resistance of hollow core slabs under vehicle fire exposure

V.K.R. Kodur [1*] and Puneet Kumar [2]

Abstract:
Prestressed hollow core concrete slabs are utilized in parking structures due to their cost effectiveness, superior quality, and inherent high fire resistance. Currently, fire resistance of these slabs is assessed based on prescriptive based approaches which are derived from standard fire tests on slabs. Vehicle fire scenarios in parking structures can be significantly different from standard or compartment fires, still there are limited guidelines to assess the fire resistance of hollow core slabs under the same. To overcome these drawbacks, a rational design approach is applied for evaluating fire resistance of hollow core slabs. A finite element based numerical model, built in ANSYS, is applied to evaluate fire performance of hollow core slabs under realistic fire loading scenarios as present in parking structures. Results from these numerical studies clearly indicate that hollow core slabs exhibit higher fire resistance under realistic fire and loading conditions.
Keywords: Hollow core slab, fire exposure, vehicle fire, finite element model, fire resistance

1 Introduction

In recent years, hollow core (HC) slabs have gained popularity due to numerous advantages they offer over traditional floor systems such as: cost-effectiveness, better space utilization, superior quality, and optimized production. One such application for HC slabs is in parking structures, where large span flooring systems are required with less columns for better space utilization. The possible vehicle fire scenario in such structures, arising from vehicle burning, can be significantly different from standard or compartment fire exposures. Typically, vehicle fires are characterized by rapid temperature rise and decay in short burning duration, whereas, standard fires include longer burning duration with no decay phase. Therefore, evaluating fire resistance based on standard fire exposure, as in prescriptive based approach, may not yield realistic fire performance assessment. Further, due to high thermal inertia of concrete, HC slabs may exhibit resistance to withstand typical short-duration vehicle fires. However, most of the previous fire resistance studies on HC slabs are based on standard fire exposure only, and there are limited guidelines to evaluate fire resistance of HC slabs under vehicle fires.

Currently, fire resistance of HC slabs is evaluated through tabulated fire ratings [1–4], which are derived from standard fire tests and are expressed in terms of equivalent slab thickness and clear cover thickness to prestressing strands. Minimum clear concrete cover to strands is provided to limit the temperature rise in prestressing strands to be below critical temperature. Similarly, minimum slab thickness is to be provided to limit temperature on the unexposed face of slab, to satisfy insulation criterion. This traditional approach of evaluating fire resistance is often conservative, and do not account for critical factors governing fire response of HC slabs. Alternatively fire resistance can be evaluated using the procedure in PCI design manual [1], where simplified calculations based on temperature dependent material degradation can recommend load carrying capacity of HC slabs at a given fire exposure time. However, no guidance for evaluating fire temperatures or cross-sectional temperatures are provided for vehicle fire scenarios for use in such simplified calculations.

[1*] Professor, Department of Civil and Environmental Engineering (*Corresponding Author), 3580 Engineering Building, Michigan State University, East Lansing, MI, USA, 48824. Tel: (+1)(517)353-9813, Fax: (+1)(517)353-9813, Email: kodur@egr.msu.edu

[2] Ph.D. Student, Department of Civil and Environmental Engineering, 3501 Engineering Building, Michigan State University, East Lansing, MI, USA, 48824. Email: kumarpu2@msu.edu

To overcome these limitations, a rational design approach is applied for evaluating fire resistance of HC slabs under vehicle fire scenario. The novelty of this approach lies in giving due consideration to realistic vehicle fire scenarios –as in typical parking structures, complex cross-sectional temperature calculations accounting for heat transfer through cores, and accounting for realistic failure limit states in evaluating fire resistance. This approach can be implemented using any commercially available finite element computer software. For this purpose, a numerical model for tracing the response of HC slabs under fire conditions is developed in ANSYS. The applicability of the proposed numerical model in tracing fire response of HC slabs under vehicle fire exposure is illustrated using a case study. Note that proposed approach is not limited to fire resistance in parking structures only, rather it provides a framework to assess fire resistance of hollow core slabs under realistic fire and loading scenarios that occur in buildings and parking structures.

2 Numerical model

A three-dimensional finite element (FE) based numerical model is developed in ANSYS [5] to implement the proposed rational design approach. The model accounts for critical factors such as: fire characteristics, member geometry, loading and support conditions, temperature dependent material properties, geometric and material non-linearity, and realistic failure limit states in evaluating fire response of HC slabs.

2.1 Analysis procedure

Fire resistance analysis of HC slab is carried out in incremental time steps from start of fire exposure to failure of the HC slab or until end of fire exposure if no failure is observed. A flow chart illustrating various steps involved in fire resistance analysis is shown in Figure 1. For the analysis, HC slab is discretized using two sets of elements, one for simulating thermal response, and the other for simulating corresponding structural response of HC slab (see Section 2.2 for details). Discretized slab can be subjected to any given fire scenario provided corresponding time-temperature history (fire temperatures) is available. Fire temperatures from selected fire scenario are provided as input to the discretized geometry in thermal domain along with other member specific thermal boundary conditions. The cross-sectional temperatures of the HC slab are calculated for the applied fire temperatures and thermal boundary conditions using a transient thermal analysis.

After completion of thermal analysis, thermal elements are converted to compatible structural elements, and service loading and support conditions are applied in terms of structural boundary conditions to the model. Numerical model allows application of all possible thermal and structural boundary conditions (in terms of convection, radiation, fixed temperatures, fixed displacements, pressure, concentrated loads etc.) as in case of real fire scenario in parking structures, and therefore, is highly versatile for HC slabs under fire exposure. The structural response of HC slab is calculated under the effect of service loading and support conditions in the first-time step of structural analysis. Stabilized displacements at the end of first time step represent typical HC slab under service loading conditions inside a parking structure.

At this stage, nodal temperatures from thermal analysis are applied as body loads, and corresponding thermo-mechanical response of HC slab is traced in incremental time steps using a coupled thermal-stress analysis. It should be noted that due to nonlinearity arising from geometrical and material behavior, convergence becomes a major problem in the analysis. Therefore, convergence of solution (see Section 2.4) is checked at each time step of analysis. Finally, the output parameters from the analysis (nodal temperatures, deflection, stress, etc.) are checked against failure limit states (see Section 2.5) at the end of each time step to evaluate fire resistance of HC slab. If one or combination of failure limit states is satisfied, the time duration to reach this failure is defined as the fire resistance of HC slab; else, incremental time steps are followed as shown in Figure 1 until failure is achieved or fire exposure duration is over.

2.2 Discretization of slab

As discussed above, HC slab is discretized into two sets of elements, one for undertaking thermal analysis and the other for structural analysis. As part of thermal analysis, the slab is discretized with SOLID70, LINK33, and SURF152 elements to simulate heat transfer between fire and slab, and within slab itself. SOLID70 is a 3D eight node element capable of modeling thermal conduction, and is used to simulate heat transfer within inner concrete layers of slab. LINK33 is two node line element which is used to model thermal conduction within prestressed strands. Unlike in solid slabs exposed to fire, where heat transfer within slab occurs through conduction alone; in case of HC slabs the heat transfer occurs through conduction as well as through convection and radiation in hollow cores. This complex heat transfer within hollow cores is captured using SURF152 elements. SURF152 is a four-node surface element capable of simulating heat transfer via conduction, convection and radiation; and is overlaid on the slab surface and inside hollow cores to simulate complex heat transfer between fire and slab, and within hollow cores.

For simulating structural response the slab is discretized with elements that can capture structural behavior. For this purpose, SOLID70 is switched to SOLID65, LINK33 to LINK180, and SURF152 to SURF154. SOLID65 element is an eight node element which is capable of simulating the cracking and crushing of concrete using William Warnke failure envelope [5], and has been successfully applied by previous researchers [6–8]. LINK180 elements are two node elements which are capable of simulating prestress, and compression or tension within steel reinforcement. SURF154 elements are utilized for the application of surface loads (pressure, displacements etc.) on the discretized geometry. All elements account for temperature dependent material and geometric non-linearities, which makes them ideal for capturing behavior of HC slab under fire. A typical HC slab, as discretized into various elements, is illustrated in Figure 2.

2.3 Material properties at elevated temperatures

It is well established that thermal and mechanical properties of concrete and steel undergo significant degradation at elevated temperatures. Therefore, to model realistic thermo-mechanical response of HC slab, temperature dependent thermal and structural material properties are to be provided as input to ANSYS [5]. Thermal properties include specific heat, thermal conductivity, and thermal expansion; whereas, elastic modulus, strength, and stress-strain relations come under mechanical properties. In the present study, variation in thermal and mechanical properties of

concrete and steel is considered to follow recommendations of Eurocode 2 [9], and temperature dependent material properties for each element are evaluated at the average nodal temperature of the element.

Due to rapid burning that can occur in vehicle fire scenarios, the convective heat transfer between fire and exposed surface of slab is significantly higher than in case of building fires. This convective heat transfer is captured using convection heat transfer coeffiecient which is assigned to SURF152 elements on the exposed face. Eurocode 1 [10] specifies a value of 50 W/m^2K (8.8 Btu/h ft^2 ^oF) for convection heat transfer coeffiecient in case of hydrocarbon fires, and 25 W/m^2K (4.4 Btu/h ft^2 ^oF) for standard building fire. However, due to lack of specific experimental data under vehicle fires a slightly conservative value of 45 W/m^2K (7.9 Btu/h ft^2 ^oF) is selected for vehicle fires. A user can use different values, provided that coefficient is known.

During structural analysis, concrete (discretized using SOLID65) is assigned a temperature dependent isotropic multi-linear material model in compression regime, whereas, tension behavior is simulated using damage based constitutive model [5]. Further, the cracking and crushing of concrete is simulated using SOLID65 as per William Warnke failure envelope [5] which requires two additional parameters viz. open and closed crack coefficients as input to ANSYS. The typical value of these parameters ranges between 0-1 with 0 representing complete loss of shear transfer (smooth crack) and 1 representing no loss of shear stress (rough crack). These parameters are assigned a value of 0.2 and 0.7, respectively. On the other hand, prestressing strands are assigned a temperature dependent kinematic hardening material model, and the prestress in strands is simulated using initial stress condition in LINK180 elements.

2.4 Numerical convergence

Incorporation of material and geometric non-linearities along with cracking and crushing of concrete at elevated temperatures will introduce significant convergence issues in the numerical model. These convergence hurdles can lead to ill-conditioned stiffness matrix, and hinder analysis in the subsequent time step. To overcome these convergence hurdles, an explicit solution scheme is utilized in capturing transient thermal response of model; which is relatively faster and more efficient than implicit scheme. In case of structural analysis, an iterative Newton-Raphson solver is utilized to capture physical thermo-mechanical response. In case, the convergence hurdle stops the FE analysis, the current load step is refined to relatively smaller increments. This is to minimize the current out-of-plane load vector norm to a small value until it can pass through specified convergence vector norms and the analysis can be resumed. However, small load increments can increase the computational effort exponentially, therefore, load steps are resumed to default value once convergence hurdle is over.

2.5 Failure limit states

HC slab can undergo failure through reaching either one or a combination of failure limit states viz. insulation, or integrity, or stability limit state. Therefore, failure of HC slab is checked against these failure limit states at the end of each time step. HC slab is said to experience failure under insulation criteria when either average temperature increase on the unexposed surface of the slab exceeds 139°C (250 °F) or temperature at any point on unexposed face exceeds 181°C (325

°F) above initial temperature [11]. Slab is said to undergo failure in integrity criteria, when the developed cracks and fissures under fire exposure allow movement of fire to the unexposed face of HC slab; thus, failing to contain fire spread.

In addition to insulation and integrity criteria, failure can occur in strength limit state i.e. moment (or shear) capacity of HC slab at a critical section falls below bending moment (or shear force) resulting from fire loading. Under prescriptive criterion, this strength limit state is not directly applied, since evaluating moment capacity at a given exposure time is quite complex. Often strength failure in prescriptive approach is evaluated based on critical temperature (427°C (800 °F)) in prestressing strands, which may not possibly represent realistic failure. As part of rational approach stresses are to be integrated across the cross-section of the slab since ANSYS output is in terms of nodal stresses. The temperature dependent flexural and shear capacity of slab is calculated, through an excel spreadsheet, as:

$$M_{nt} = \sum \sigma_{zT} A_e d_{naT}$$

$$V_{nt} = \sum \tau_{yzT} A_e$$

Where, M_{nT} and V_{nT} represent temperature dependent flexural and shear capacity of slab, A_e is cross-sectional area of individual element, σ_{zT} is normal stress, τ_{yzT} is shear stress along transverse direction of slab, d_{naT} is distance of centroid of element to neutral axis of the slab under fire conditions.

In addition to the above limit states, British Standard BS 476 [12] specifies deflection or deflection rate as a possible failure limit state for horizontal members (beams or slabs). Based on BS 476 [12] criteria, failure occur when the maximum deflection in the member exceeds L/20 at any fire exposure time, or the rate of deflection exceeds the limit given by $L^2/9000d$ (mm/min) after attaining a maximum deflection of L/30, where, L = span length of the slab (mm), and d = effective depth of the slab (mm). This limit state was also considered in evaluating failure by comparing deflection predictions output by ANSYS at any given time step with corresponding deflection limit.

3 Model validation

The above numerical model is validated against data from fire tests on two full-scale HC slabs exposed to two different fire scenarios [13]. Thermal and structural predictions from the model are compared with measured values to gauge the efficacy of proposed model in tracing fire response of HC slab.

3.1 Slab details

Two tested slabs were selected from PCI design manual [1] (4HC8-78S), and were fabricated using concrete extrusion process in a fabrication plant to meet specifications of commercially produced slabs. In this process, extrusion die of desired HC slab configuration (200 mm (7.9 in) deep with six 150 mm (5.9 in) hollow cores) is run over a 150 m (492.1 ft) long casting bed. Seven

12.7 mm (0.5 in) diameter prestressing strands were laid on the casting bed at a clear cover of 44 mm (1.7 in), which were stretched using hydraulic jacks at ends of casting bed to produce a prestressing force equivalent to 70% tensile strength of strands. The concrete mix was fed continuously to extrusion die using a hopper, and continuous HC slab cross-section was extruded by forcing the concrete through vibrating die. Proper compaction of concrete was ensured by vibrating die, and lubricated casting bed enabled easy stripping of slabs. HC slab lengths of 4 m (13.1 ft) were cut using wet saw for slab 1 and slab 2 after 10 hours of casting, when concrete strength measured 35-37 MPa (5-5.3 ksi). The strength of concrete at the day of fire testing measured 75 MPa (10.9 ksi) for both slab 1 and slab 2. The slabs were cured for about 10 months, and then tested under fire conditions.

Both slabs were tested under four-point loading scheme, with simply supported conditions and a constant load level of 69.4 kN (15.6 kip) (equivalent to 60% of the room temperature capacity), see Figure 3. Slab 1 was tested under standard fire exposure (ASTM E119) and slab 2 was tested under design fire scenario, as illustrated in Figure 4. The design fire consisted of a two hour burning phase and a cooling rate of 10^{o}C /min, which represents a typical severe ventilation controlled fire. The ends of hollow cores were not sealed during fire testing to represent accurate service conditions of HC slabs, and fire response of HC slab was measured in terms of cross-sectional temperatures, mid-span deflections, and failure modes. Details of the selected HC slabs for validation are provided in Table 1.

3.2 Analysis details

The above numerical model is applied to analyze slab 1 and 2 under identical loading and boundary conditions as in fire tests [13]. To save the computational effort, the steel beams at the ends, used for providing simply supported conditions, are replaced with simple boundary conditions in the analysis. Further, due to symmetry in loading, geometry, material properties, and boundary conditions only half-symmetric model of the HC slab is analyzed for both slabs. The symmetric boundary condition is implemented by constraining the out-of-plane displacement and rotation degree of freedoms at the plane of symmetry (at the mid span). These simplifications significantly reduce the number of elements required for discretization of slabs, and lead to swift analysis with high computational efficiency. The half-symmetric model of HC slab 1 and 2 is analyzed as per procedure laid out in Section 2.

3.3 Thermal response

Comparison between predicted and measured temperatures at various cross-sectional depths of slab 1 and slab 2 is illustrated in Figure 5. Overall, both slabs follow similar temperature progression trends, and model predictions are in good agreement with measured temperatures. The temperature rise in prestressing strands is at slow pace as compared to temperatures on the exposed face due to effect of high thermal inertia of concrete. In the first 20 min of fire exposure, temperatures at various depths within HC slab raise slowly, after 20 min, temperatures raise at moderate pace. As expected, temperatures near exposed face of HC slab are higher than those close to unexposed face. Measured cross-sectional temperature in slab 1 range between 205 ^{o}C (401 ^{o}F) to 456 ^{o}C (852 ^{o}F), and between 197 ^{o}C (386 ^{o}F) to 393 ^{o}C (739 ^{o}F) for slab 2 at the end of fire exposure. Slightly lower temperatures in slab 2, relative to slab 1, are measured due to the presence

of decay phase and relatively lower fire temperatures in design fire scenario which is utilized for fire exposure in slab 2. The decay phase in design fire starts at 120 min with a cooling rate of 10 ^{o}C/min (50 ^{o}F/min), however, the effect of decay phase is observed from small drop in strand temperatures at near 130 min (see Figure 5(b)) and temperatures at mid-depth and unexposed face do not show any decrease in temperature. This is attributed to high thermal inertia of concrete as well which do not allow rapid cooling of HC slab.

For both slabs, temperature predictions in prestressing strands are slightly higher than measured values, whereas, temperatures at mid-span are under predicted. On the other hand, predicted temperatures at unexposed face are very close to measured values in the first 20 min, followed by under predicted, good correlation, and then slightly over predicted for both slabs. This variation in predicted and measured temperatures is primarily due to variation in the actual and code provisions for material properties of concrete and strands at elevated temperature. Further, significant longitudinal cracking was observed on the exposed face in the fire tests of slab 1 and 2. Such longitudinal cracks in hollow cores near exposed face have high potential to allow hot fire gases to pass through cracks, and increase the heat transfer within cores [13]. Currently, the proposed model does not account for this effect of cracking on heat transfer within cores, due to lack of compatible elements which can capture two-way coupling between thermal and structural analysis. Therefore, once the cracking in hollow cores allows hot gases through, the temperatures are under-predicted at mid-depth of HC slab.

3.4 Structural response

Structural response is validated by comparing predicted deflections against measured values. Figure 6 illustrates a comparison between measured and predicted mid-span deflections for slab 1 and slab 2. The mid-span deflection response for both slabs can be grouped into three main stages. In the first stage (0-20 min), the mid-span deflections result from thermal expansion and increase at a slow pace due to slow raise in cross-sectional temperatures as illustrated in Figure 5. After 20 min, in stage 2, mid-span deflection raises at a moderate pace due to significant degradation in mechanical properties of concrete and strands arising from moderately raising cross-sectional temperatures. Finally, after 80 min of fire exposure deflections start to increase rapidly due to combined effects of cracking, significant material degradation, and creep effect. The prestressing strand temperatures in this stage range between 365-550 ^{o}C (689-1022 ^{o}F), and surpass critical temperature of 427 ^{o}C (800 ^{o}F) in strands at which prestressing strands loose approximately 50% of their room temperature strength; hence, lead to significant material degradation.

Overall, there is good correlation between predicted and measured values for both slabs in stage 1 and 2. However, model over predicts deflections in the third stage. This can be attributed to the early yielding of prestressing strands due to slightly over predicted strand temperatures, and smeared cracking in SOLID65. As discussed in Section 3.3, strand temperatures are slightly over predicted by model, which causes early yielding of prestressing strands as compared to fire tests. Also, significant cracking of HC slab occurs in the third stage, and long discrete cracks running through the length of hollow cores or across the cross-section are observed in fire tests. Such discrete cracks tend to form cracked and un-cracked zones within HC slab, and do not transfer stresses to the un-cracked sections of HC slabs. However, SOLID65 simulates smeared cracking of HC slab, where cracks are smeared over entire element unlike actual localized discrete cracking

of concrete as observed in fire tests. This smeared cracking in SOLID65 elements continue to transfer stresses to untracked portions of HC slab, and allows un-cracked sections to experience relatively higher stresses than in fire tests which contributes to over predicted deflections in third stage for both slabs.

3.5 Failure time and failure mode

A comparison between predicted and measured failure times and modes is illustrated in Table 2. The main failure mechanism of the HC slabs was failure under insulation limit state. This is due to convection and radiation heat transfer in hollow cores of HC slab, which allows faster transmission of temperatures to the unexposed face as compared to solid slab. Slab 1 reached insulation limit state (temperature rise of 181 ^{o}C (325 ^{o}F)) at 120 min, whereas, slab 2 reached insulation limit state at 145 min. Model correctly predicts the failure times and mode for both slabs in insulation limit state, with an error of 9.1% for slab 1 (109 min) and 8.9 % for slab 2 (132 min). Lower failure time of slab 1 in insulation limit state is attributed to relatively severe ASTM E119 fire exposure as compared to design fire exposure subjected to slab 2. High fire temperatures of ASTM E119 fire exposure causes fast transmission of temperatures within HC slab, as compared to low temperatures with decay phase in design fire exposure, and therefore, insulation limit state is attained earlier in slab 1.

Slabs did not fail under integrity criteria as flame did not breach through unexposed face of slabs. Also, both slabs continued to carry applied loading beyond insulation failure, and ultimate failure of slab 1 occurred at 140 min due to excessive flexural cracking, whereas, no failure in strength domain was observed for slab 2. Deflection limit state predicts higher fire resistance for both slabs (122 min for slab 1, and 135 min for slab 2) indicating HC slabs continue to carry load even after the failure in insulation limit state, as observed in fire test. Also, model predicts ultimate failure of HC slab under flexural limit state with excessive flexural cracking and deflection, which was observed experimentally as well. Overall, there is reasonable agreement between model predictions and test data under standard and design fire scenario, and therefore, proposed model can be utilized to trace the fire response of HC slabs.

4 Case study

A case study is carried out to illustrate the applicability of the rational methodology in evaluating fire resistance of typical HC slab present in a parking structure. The fire resistance analysis is carried out using the above developed numerical model in ANSYS.

4.1 Selection of slab and fire exposure scenario

Slab 1, designated 4HC8-78S in PCI design manual, with a maximum permissible span of 12.2 m (40 ft) is selected for the analysis. The geometry, material, and loading and boundary conditions of slab 1 are kept similar to that in Section 3, which induce a load ratio of 60% (typical load ratio in parking structures) within HC slab. Fire resistance analysis is carried out on this slab by exposing it to two typical vehicle fire scenarios that can occur within a parking structure.

One of the biggest challenges in analyzing fire resistance under vehicle fire scenario is to identify the appropriate fire scenario i.e. how many cars are involved in fire, the location of fire, and resulting fire temperatures. Critical vehicle fires in parking structures use scenarios as shown in Figure 7 [14]. Fire temperatures in vehicle fire scenario are characterized by number of vehicles involved in fire, and a detailed discussion on progression of fire temperatures in various vehicle fire scenarios can be found in the literature [15,16]. Out of these, scenario 1 and 5 encompass more than 98.7% of possible vehicle fires in parking structures [14,17]. Therefore, to investigate the behavior of HC slabs under vehicle fire exposure, fire temperatures are considered as per full scale experimental study of Zhao and Kruppa [18]. The resulting vehicle fire temperatures from scenario 1 and 5 are presented in Figure 4. In Figure 4, Parking Fire 1 represents fire scenario 5 involving three vehicles placed right next to each other where fire propagates from middle car to both cars in the proximity. Whereas, Parking Fire 2 represents a scenario 1 type vehicle fire which do not propagate to nearby vehicles. Vehicle fire scenarios with less number of vehicles (Parking Fire 2) tend to burn out quickly as in case of hydrocarbon fires, whereas, vehicle fire scenarios with two or more vehicles (Parking Fire 1) represent delayed peak temperatures and longer burning durations as fire progresses from one vehicle to other (see Figure 4).

Together, these fire scenarios encompass more than 98.7% of possible vehicle fires, and therefore, provide a comprehensive case study on vehicle fires in a parking structure. Further, entire bottom portion of slab is exposed to the fire (as per temperature-time relations shown in Figure 4), instead of selecting localized fire. This is to be on the conservative side, as there can be significant uncertainty associated with the location of vehicle fire. On the other hand, standard fire scenario involves use of ASTM E119 fire curve [11], as shown in Figure 4. Therefore, discretized geometry of slab 1, as discussed in Section 3.2, is analyzed under standard and two critical vehicle fire exposures.

4.2 Thermal response

Progression of cross-sectional temperatures in HC slab under vehicle and standard fire exposures (ASTM E119 fire) is illustrated through Figures 5(a), 8 and 9. The effect of thermal inertia of concrete is more pronounced in case of vehicle fire exposure, and can be clearly observed from Figure 8. In case of Parking Fire 1, the fire temperatures increase slowly in the beginning till 25 min, and then peak fire temperatures are attained in between 25-55 min, followed by a decay phase. Due to slow rise in fire temperatures until 25 min of fire exposure, cross-sectional temperatures within slab are almost unaffected in the initial 30 min of fire exposure, and then increase at a moderate pace for all depths. Prestressing strands attain a peak temperature of 178 ^{o}C (352 ^{o}F), and decay in strand temperature starts at a time lag of 30 min from the start of decay phase in fire temperatures. Progression of temperatures at inner depths of slab is at much slower pace, as compared to strand temperatures, and with higher time lags relative to occurrence of decay phase in fire temperatures due to effect of thermal inertia of concrete.

In case of Parking Fire 2, the fire temperatures increase rapidly and attain peak temperatures within 15 min of fire exposure, followed by a decay phase. Therefore, unlike Parking Fire 1, there is no time lag for increase in cross-sectional temperatures, and temperatures increase at all depths at a moderate pace from the start of fire exposure itself. Prestressing strands reach a peak temperature of 140 ^{o}C (284 ^{o}F) at a time lag of 45 min from the start of decay phase in fire

temperature. This higher time lag in occurrence of peak temperatures is observed due to rapid heating of slab in the initial duration of fire exposure, which does not allow ample time to overcome thermal inertia of concrete. Therefore, it takes longer for HC slab to reach peak temperatures under Parking Fire 2 exposure. Similar to Parking Fire 1, progression of temperatures at inner depths of slab is slower than strand temperatures and at a higher time lag from occurrence of decay phase in fire temperatures.

It should be noted that cross-sectional temperatures maintain well below 200 ^{o}C (392 ^{o}F) for both vehicle fire exposures. In case of standard fire, the cross-sectional temperatures inside HC slab are below 200 ^{o}C (392 ^{o}F) until 37 min of fire exposure as well; however, due to the absence of decay phase in standard fire, the cross-sectional temperatures continue to raise. It can be clearly observed from Figure 9 that under standard fire exposure temperatures in strands and on unexposed face are much higher as compared to vehicle fire scenario. While temperatures from vehicle fire scenario are well below limiting temperature, still temperatures under standard fire scenario surpass limiting temperature criteria suggesting failure of slab as per prescriptive approach. Therefore, it is vital to incorporate decay phase in vehicle fire exposure for realistic fire performance evaluation of HC slab.

4.3 Structural response

The structural response of HC slab under vehicle and standard fire exposure can be evaluated by looking at progression of deflections, as well as degradation in load carrying capacity with fire exposure time. Comparison of degradation in moment and shear capacity of slab is shown in Figures 10 and 11, and progression of mid-span deflections is illustrated in Figure 12. It can be clearly observed from Figure 10 that standard fire exposure (ASTM E119) leads to significantly high degradation in moment capacity as compared to vehicle fire exposure. Moment capacity under standard fire exposure degrades below applied moment at 109 min of fire exposure, suggesting possible failure of slab in strength limit state. However, the degradation in moment capacity under vehicle fire exposure is almost negligible as compared to that of standard fire exposure. Moment capacity degradation attains peak value at an earlier fire exposure time under Parking Fire 2 than as compared to Parking Fire 1 exposure. This is due to lag in the rise of cross-sectional temperatures in the initial 30 min of fire exposure for Parking Fire 1, as explained in previous section. However, the peak degradation under Parking Fire 1 exposure is relatively higher than that of Parking Fire 2 exposure, which is due to higher cross-sectional temperatures under Parking Fire 1 exposure (see Figure 8).

Degradation in shear capacity of slab is relatively small under vehicle fire exposure as compared to standard fire exposure, and Parking Fire 1 exposure causes higher degradation in shear capacity as compared to Parking Fire 2 exposure with a small time lag between the occurrences of the same. It should be noted that shear capacity degradation starts at an early fire exposure duration relative to moment capacity degradation under all three fire exposures. This is due to significantly less area of cross-section of HC slab due to presence of hollow cores, which makes HC slabs prone to failure in shear limit state. However, shear failure was not observed under any selected fire exposure due to low cross-sectional temperatures.

In case of deflection response, a similar trend of degradation in moment capacity is observed. Failure in deflection limit state is observed under standard fire exposure at 122 min, whereas, deflection under vehicle fire exposure is almost negligible relative to that of standard fire exposure. Parking Fire 1 causes higher peak deflection relative to Parking Fire 2 at a small time lag, as in case of degradation in moment and shear capacity. Therefore, parking fires with higher temperatures and longer burning duration produce higher fire severity. Further, slab undergoes failure in strength limit state under standard fire exposure alone, and degradation in load carrying capacity and mid span deflection under vehicle fire scenario is relatively negligible as compared to standard fire scenario. In case of vehicle fire scenario, the effect of cooling phase can be clearly observed in the structural response; as degradation in load carrying capacity and mid-span displacements stabilize after attaining peak values and do not reach limiting criterion. However, in case of standard fire exposure, temperatures keep increasing until ultimate failure is achieved. Therefore, it is important to consider the effect of cooling or decay phase in vehicle fire scenarios.

4.4 Failure times and failure modes

A comparison between the predicted failure time and failure modes under vehicle and standard fire exposure is illustrated in Table 3. It should be noted that the HC slab fails under standard fire scenario alone and no failure occurs under vehicle fire scenario. Standard fire exposure leads to failure of HC slab at 109 min under insulation limit state, 122 min under deflection limit state, 85 under prescriptive strand limiting temperature criterion, and at 109 min under strength (moment) limit state. Therefore, standard fire exposure predicts a fire resistance of 85 min for the slab, whereas, prescriptive codes specify a fire resistance of 90 min for the same slab [1,2,9]. However, application of rational approach yields no failure under vehicle fire exposure. This clearly illustrates the over conservative behavior of prescriptive approach which can lead to costly designs.

5 Design implications

Currently, fire resistance of HC slabs is evaluated based on prescriptive based approach which is derived from standard fire tests. These tests are expensive, time consuming, and do not yield realistic assessment of fire performance. An alternative to this is the use of rational design methodology. Currently, there are limited guidelines to assess the fire resistance of HC slab using rational approach. The current rational approaches outlined in some design manuals [1] to evaluate fire resistance of HC slabs do not account for critical factors governing fire response of HC slabs and may not provide accurate fire performance assessment of HC slabs.

A numerical model capable of tracing the behavior of HC slabs from pre-fire stage to collapse under realistic fire and loading conditions is developed in ANSYS. This model accounts for critical factors governing fire response of HC slabs, and has been utilized to implement rational design approach for fire resistance evaluation of HC slabs under typical vehicle fire exposures in parking structure. The results of this study clearly demonstrate that fire resistance of HC slabs is significantly undermined by prescriptive based approach. Further, this approach can be implemented using any commercial finite element based software, such as ANSYS in this study. Therefore, use of this approach integrates fire resistance design with structural design, and gives the freedom to designers to optimize their design without the need for costly fire tests. Also, it

allows user to perform a series of parametric studies to understand the effect of design parameters on fire resistance of HC slabs. Results from such parametric studies can be utilized to develop rational and cost-effective design guidelines for incorporation into codes and standards, and are currently under progress at Michigan State University.

6 Conclusions

The application of rational design approach for fire resistance evaluation in HC slabs under vehicle fire exposure is illustrated through a case study in this paper. Based on the information presented in this paper, following conclusions can be drawn:

1. Proposed numerical model in ANSYS can be utilized to trace the fire resistance of HC slabs with reasonable accuracy from pre-fire stage to collapse stage.
2. Using limiting temperature in prestressing strands as failure criteria in strength limit state, as in prescriptive approach, does not represent realistic fire resistance assessment.
3. Parking fires with high peak temperatures and longer burning duration represent more severe fire scenario as compared to parking fires with rapid increase in fire temperatures and shorter burning duration.
4. It is vital to account for decay phase (natural decrease in fire temperatures during realistic vehicle fires) in fire resistance evaluation of HC slabs under vehicle fire exposure, which is not accounted for in the standard fire testing.
5. HC slabs perform very well under realistic vehicle fire exposure, and fire resistance is significantly undermined by prescriptive based approach.

References

[1] PCI Industry Handbook Committee (2004). PCI Design Handbook: Precast and Prestressed Concrete, Sixth Edition.

[2] ACI Committee 216 (2007). ACI 216.1-07, Code requirements for determining fire resistance of concrete and masonry construction assemblies, Farmington, MI: American Concrete Institute.

[3] Fire Subcommittee of the PCI Building Code (2011). Design for Fire Resistance of Precast/Prestressed Concrete, PCI MNL-124, Third Edition.

[4] International Code Council (2015). International Building Code, Chapter 7: Fire and Smoke protection Features.

[5] ANSYS (2015). Mechanical APDL theory reference, Version 16.2. Canonsb ANSYS, Inc.

[6] Kodur, V. K. R., Naser, M., Pakala, P., & Varma, A. (2013). Modeling the response of composite beam–slab assemblies exposed to fire. Journal of Constructional Steel Research, 80, 163-173.

[7] Hawileh, R. A., El-Maaddawy, T. A., & Naser, M. Z. (2012). Nonlinear finite element modeling of concrete deep beams with openings strengthened with externally-bonded composites. Materials & Design, 42, 378-387.

[8] Kumar, P. (2015). “Characterization of in-plane and out-of-plane behavior of infill panels subjected to thermal exposure. Master’s Thesis, Department of Civil Engineering, IIT Gandhinagar.

[9] Eurocode 2 (2004). Design of concrete structures, Part 1-2: General rules-structural fire design, ENV 1992-1-2, UK: CEN: European Committee for Standardization.
[10] Eurocode 1 (2002). Actions on structures—Part 1-2: General actions—Actions on structures exposed to fire, UK: CEN: European Committee for Standardization.
[11] ASTM (2016). Standard test methods for fire tests of building construction and materials, E119-16a, American Society for Testing and Materials, West Conshohocken, PA.
[12] European Committee for Standardization (1987). BS 476-20, Fire tests on building materials and structures part 20, Brussels, Belgium.
[13] Shakya, A. M., & Kodur, V. K. R. (2015). Response of precast prestressed concrete hollowcore slabs under fire conditions. Engineering Structures, 87, 126-138.
[14] Haremza, C., Santiago, A., & da Silva, L. S. (2013). Design of steel and composite open car parks under fire. International Journal of Advanced Steel Construction, 9(4), 350-368.
[15] Li, Y. (2004). Assessment of vehicle fires in New Zealand parking buildings, Master's Thesis, University of Canterbury, New Zealand.
[16] Li, Y., & Spearpoint, M. (2007). Analysis of vehicle fire statistics in New Zealand parking buildings. Fire technology, 43(2), 93-106.
[17] Joyeux, D., Kruppa, J., Cajot, L. G., Schleich, J. B., Van de Leur, P., & Twilt, L. (2002). Demonstration of real fire tests in car parks and high buildings. EUR, (20466), 1-171.
[18] Zhao, B., & Kruppa, J. (2004). Structural behaviour of an open car park under real fire scenarios. Fire and materials, 28(2-4), 269-280.

Unit conversion

U.S. Unit	**SI Conversion**
1 inch	25.4 mm
1 foot	0.3048 m
1 ksi	6.89 MPa
X ^{o}F	(X-32) (5/9) ^{o}C

Table 1 Geometric and material properties of hollow core slabs selected for validation

Parameter	Slab 1	Slab 2
Dimensions (m)	4 x 1.2 x 0.2	4 x 1.2 x 0.2
Cores	Six 150 mm φ cores @ 187 mm c/c	Six 150 mm φ cores @ 187 mm c/c
Fire exposure	ASTM E119	Design fire
Failure mode	Flexural cracking	No failure
Concrete strength-test day (MPa)	75	75
Aggregate type	Calcareous	Calcareous
Prestressing strands (low relaxation)	Seven – 12.7 mm φ strands	Seven – 12.7 mm φ strands
Strand strength (MPa)	1860	1860
Clear cover to prestressing strands (mm)	44	44
Load ratio (% of capacity)	60	60

Table 2 Measured and predicted failure times of slabs

Selected slab	Failure time (min)		% Difference	Mode of failure (test and model)
	Measured	Predicted		
Slab 1	120	109	9.1	Insulation limit state
Slab 2	145	132	8.9	Insulation limit state

Table 3 Comparison of failure times under standard and vehicle fire exposures

Failure Limit State	Standard Fire	Vehicle Fire	
	ASTM E119 (min)	Parking Fire 1 (min)	Parking Fire 2 (min)
Insulation	109	No failure	No failure
Deflection	122	No failure	No failure
Strength (Strand Temperature)	85	No failure	No failure
Strength (Moment Capacity)	109	No failure	No failure
Strength (Shear Capacity)	No failure	No failure	No failure

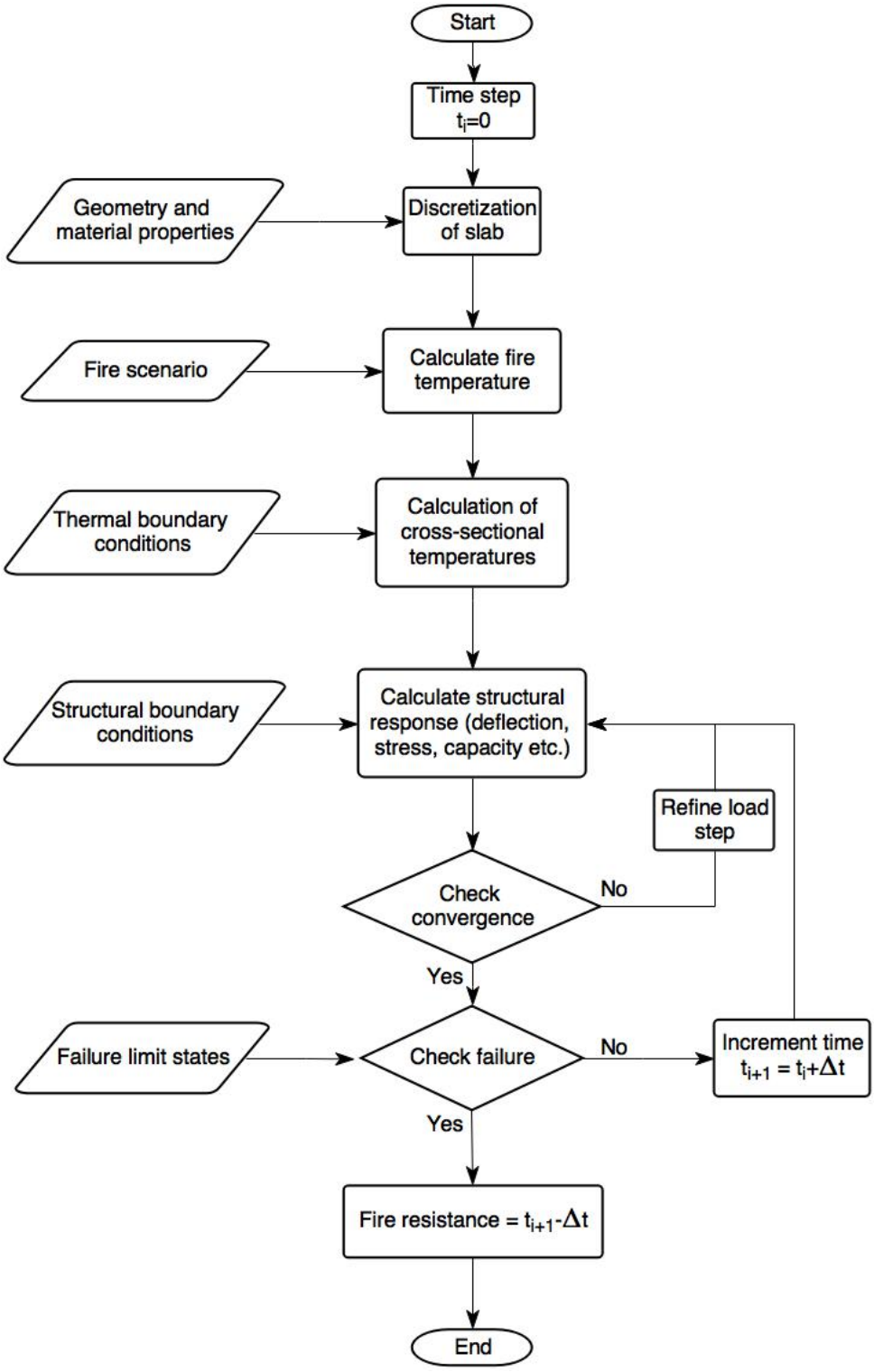

Figure 1 Flowchart illustrating steps involved in fire resistance evaluation of HC slabs

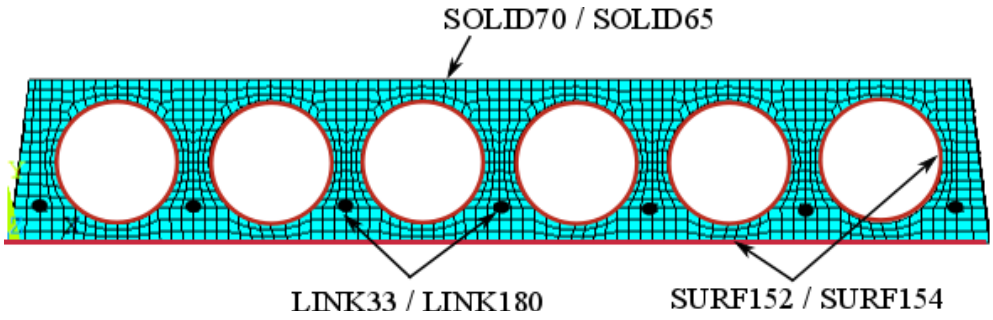

(a) Discretized cross-section of HC slab

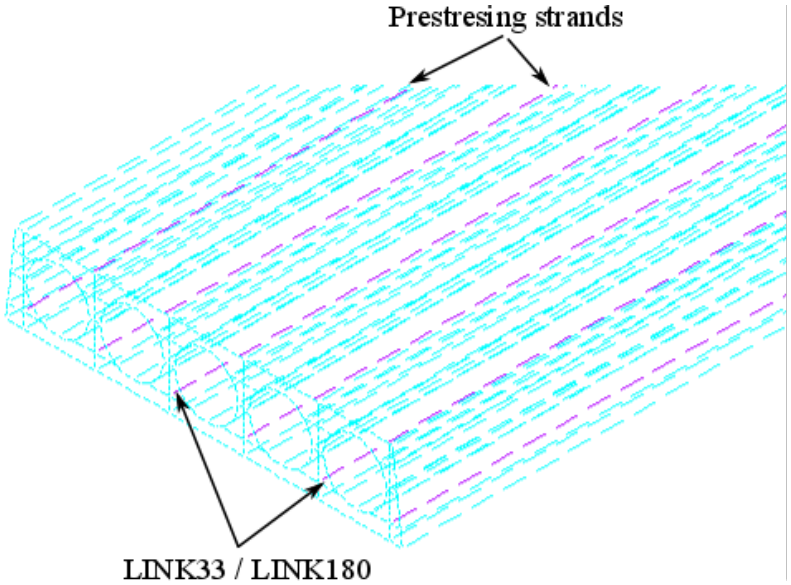

(b) Longitudinal view of discretized prestressing strands in HC slab

Figure 2 Discretized HC slab in ANSYS

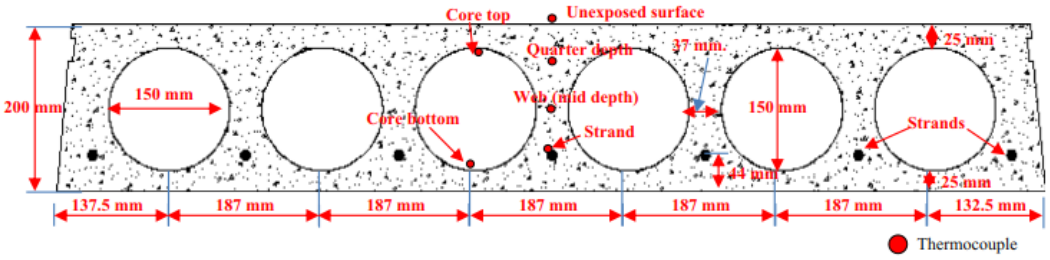

(a)

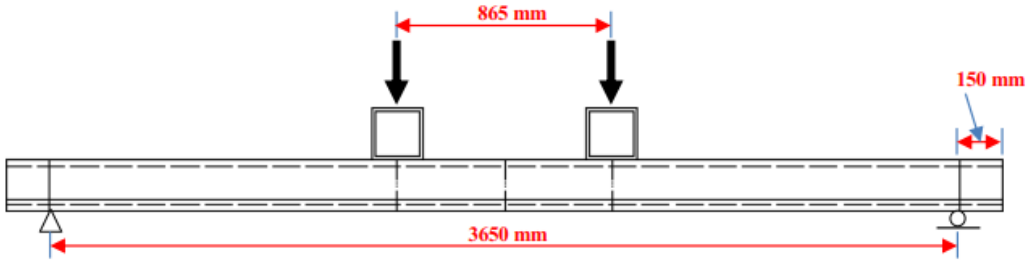

(b)

Figure 3 (a) Layout and cross-sectional details of slab 1 and slab 2, and (b) four-point loading scheme for fire resistance testing slab [13]

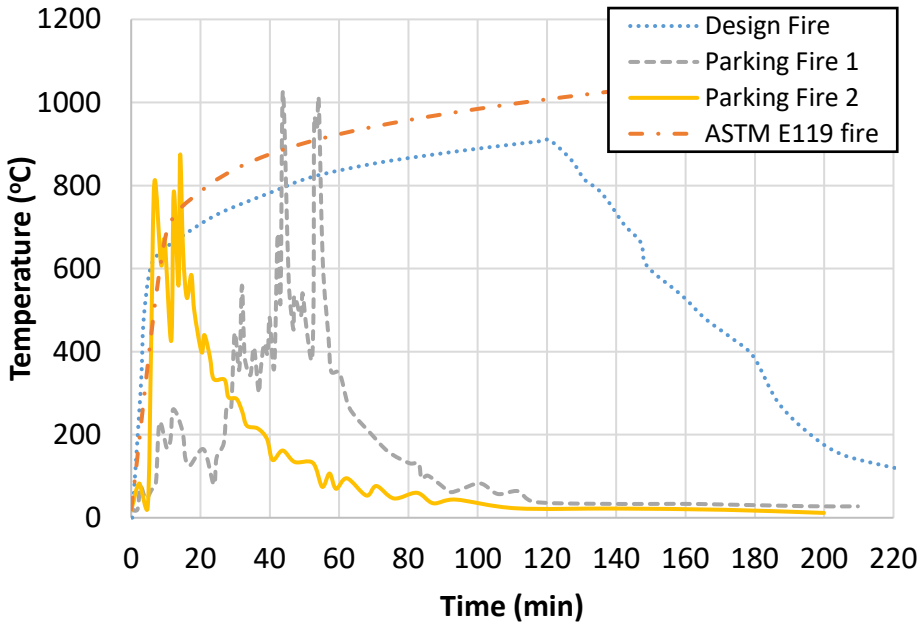

Figure 4 Time-temperature history for standard, design, and vehicle fire scenarios

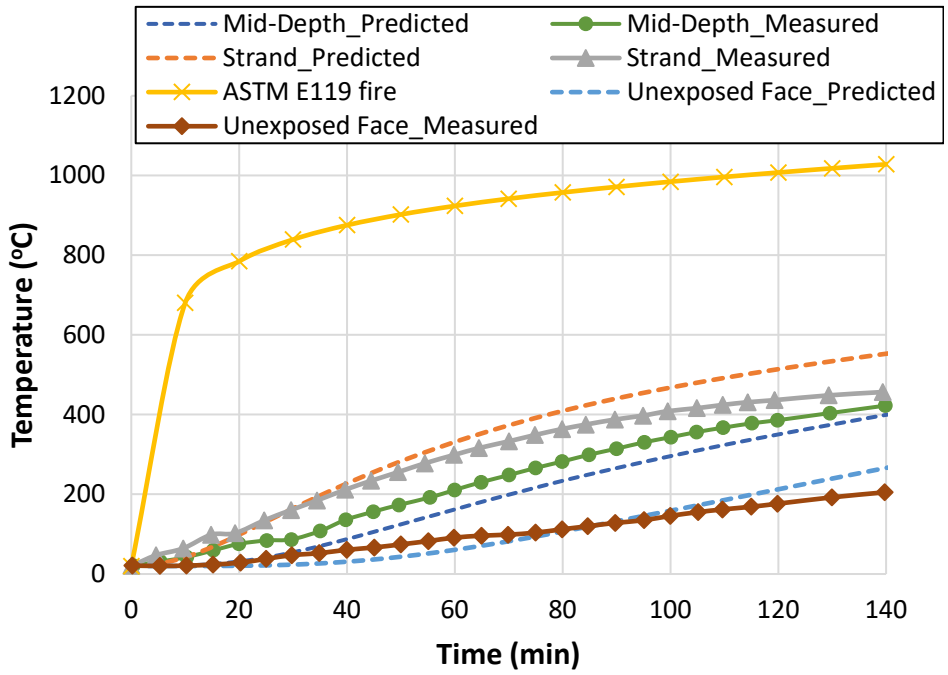

(a) Slab 1

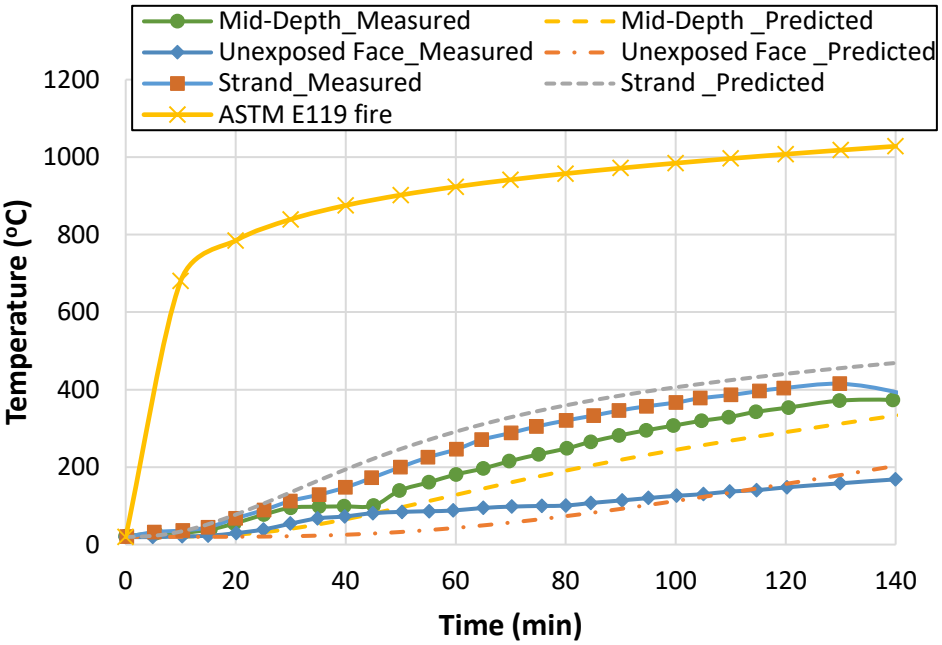

(b) Slab 2

Figure 5 Comparison between predicted and measured temperatures

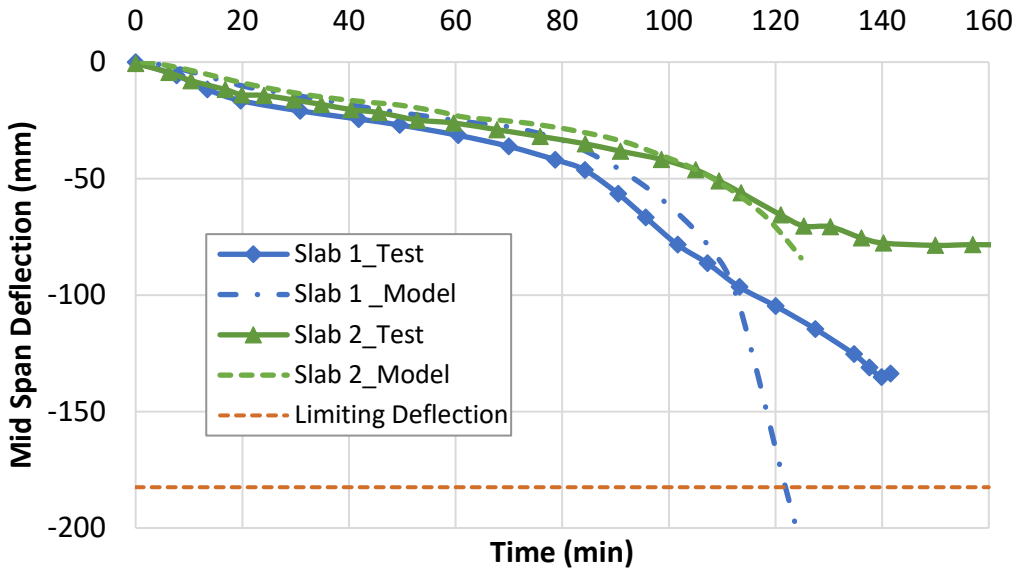

Figure 6 Comparison between predicted and measured mid-span deflections

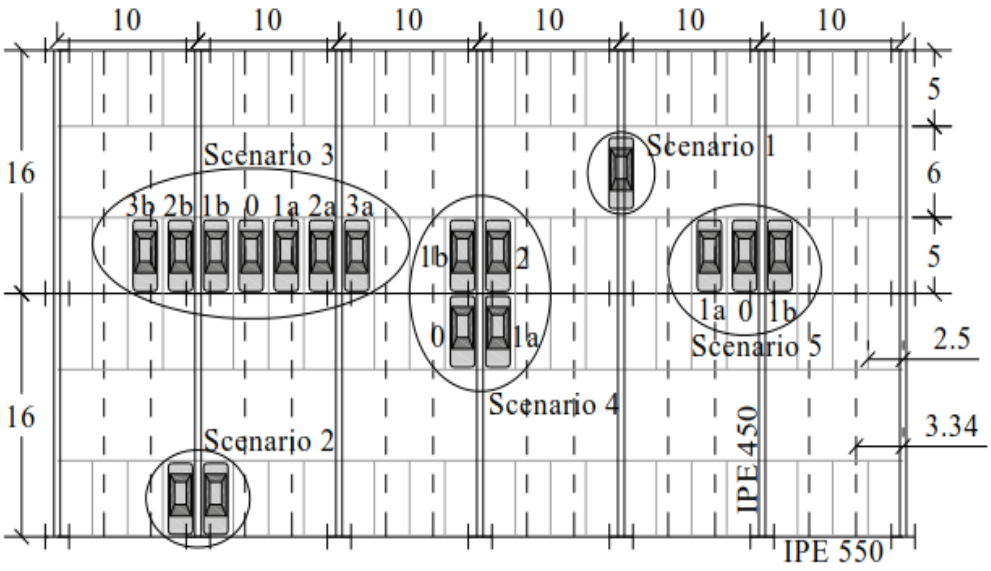

Figure 7 Critical fire scenarios that can occur in a parking structure due to burning of vehicles [14]

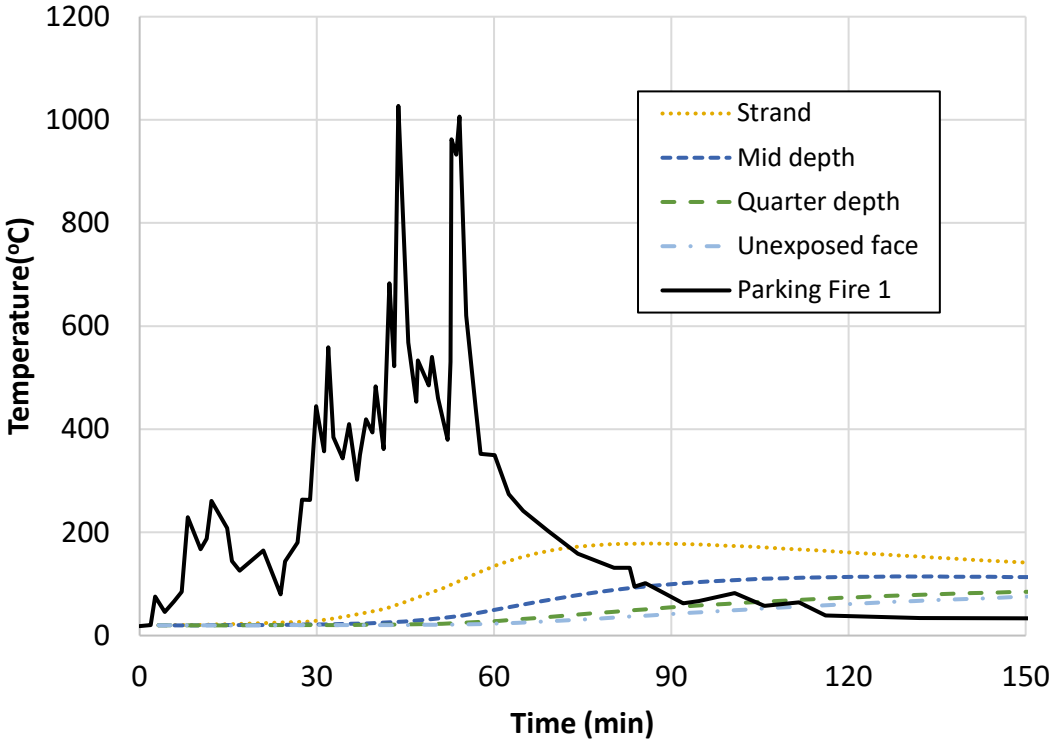

(a) Parking Fire 1

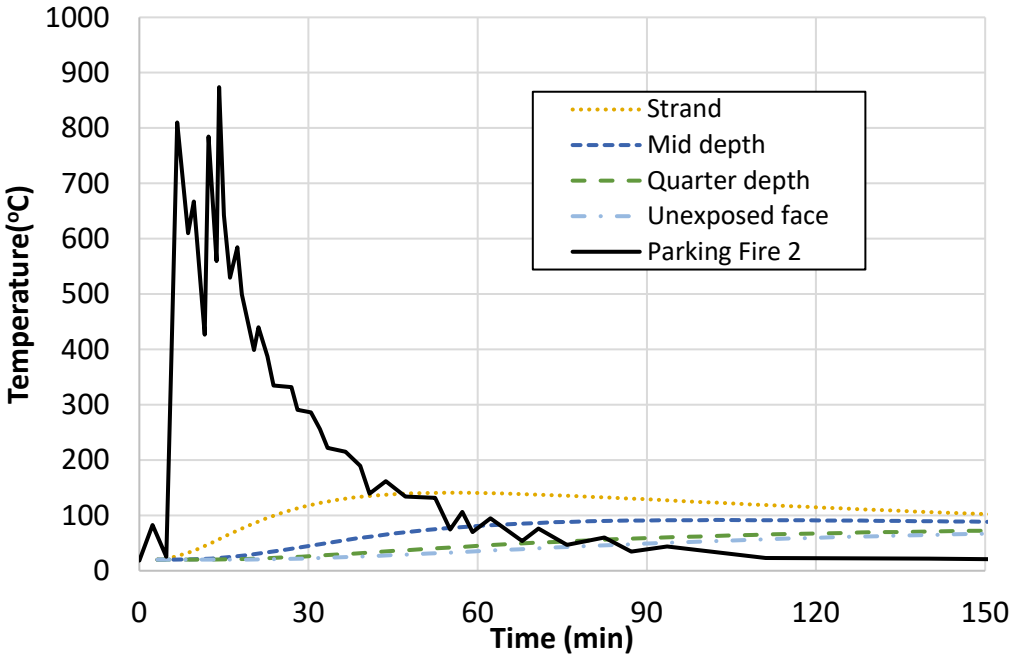

(b) Parking Fire 2

Figure 8 Cross-sectional temperatures in HC slab 1 as a function of fire exposure time

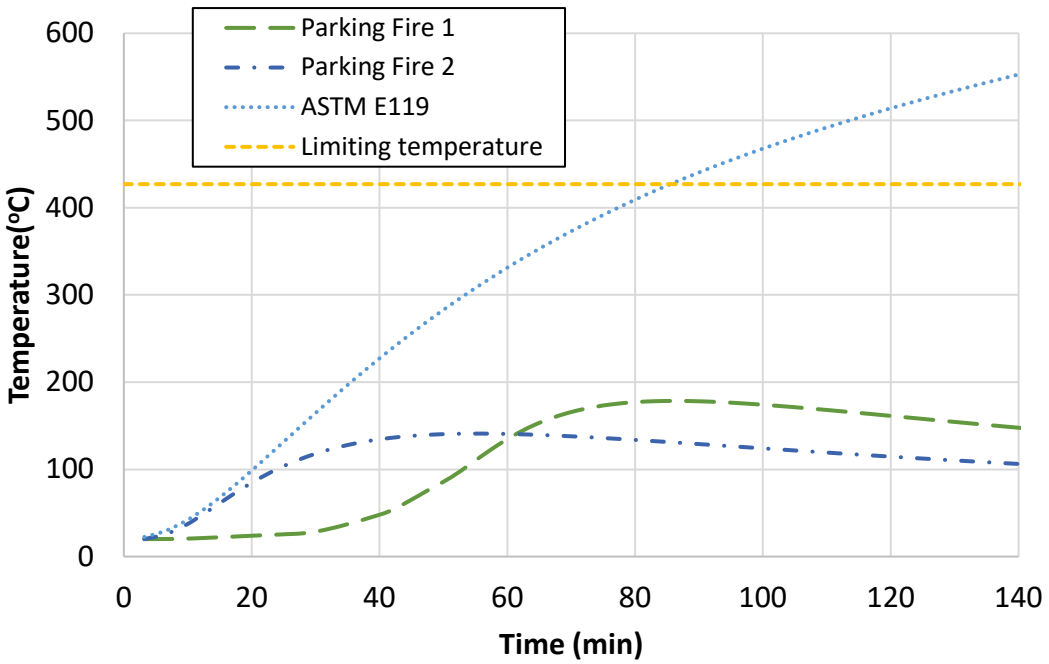

(a) Prestressing strands

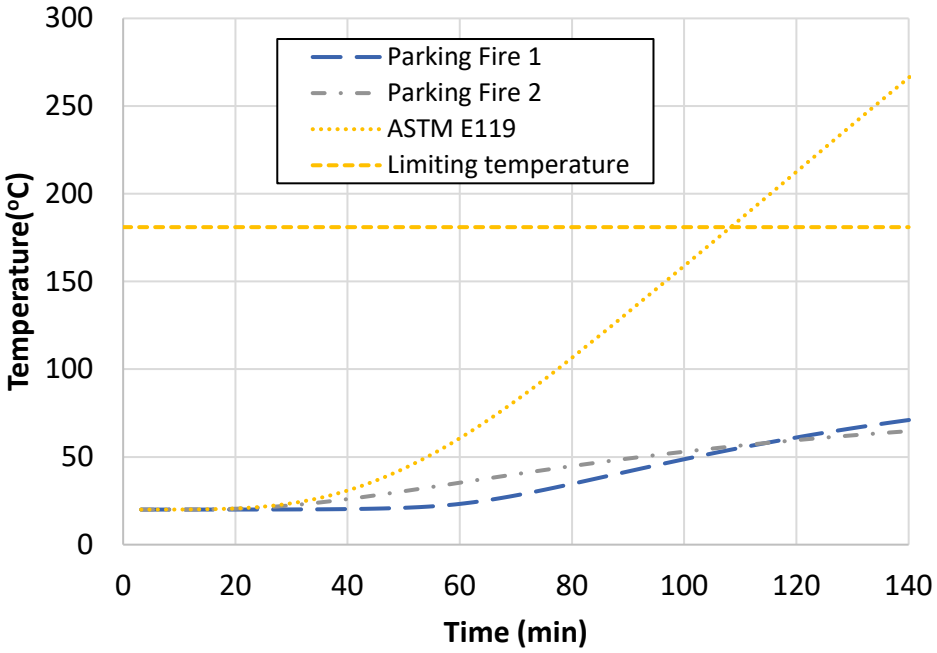

(b) Unexposed face

Figure 9 Comparison of temperatures under standard and vehicle fire scenario

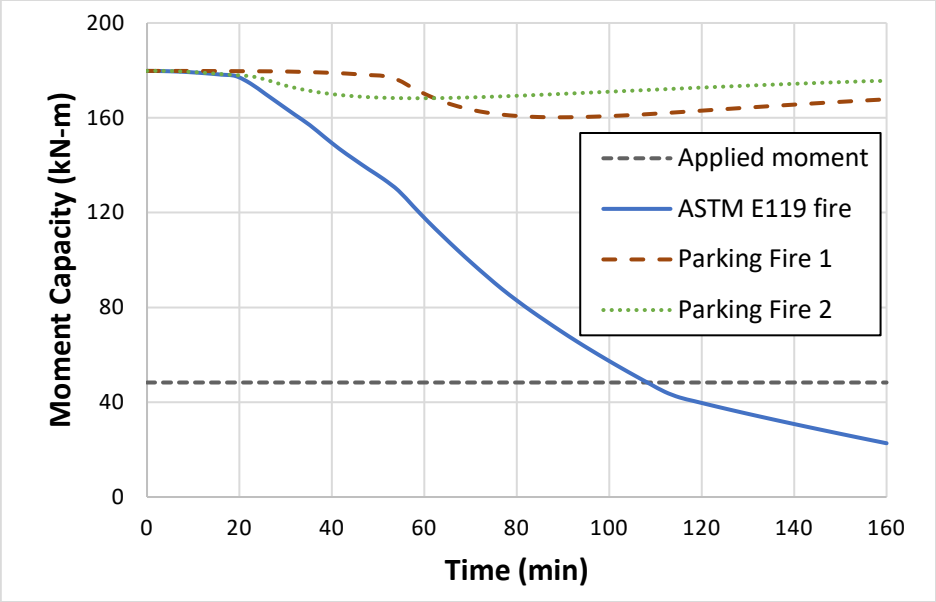

Figure 10 Comparison of degradation in moment capacity under standard and realistic fire scenario

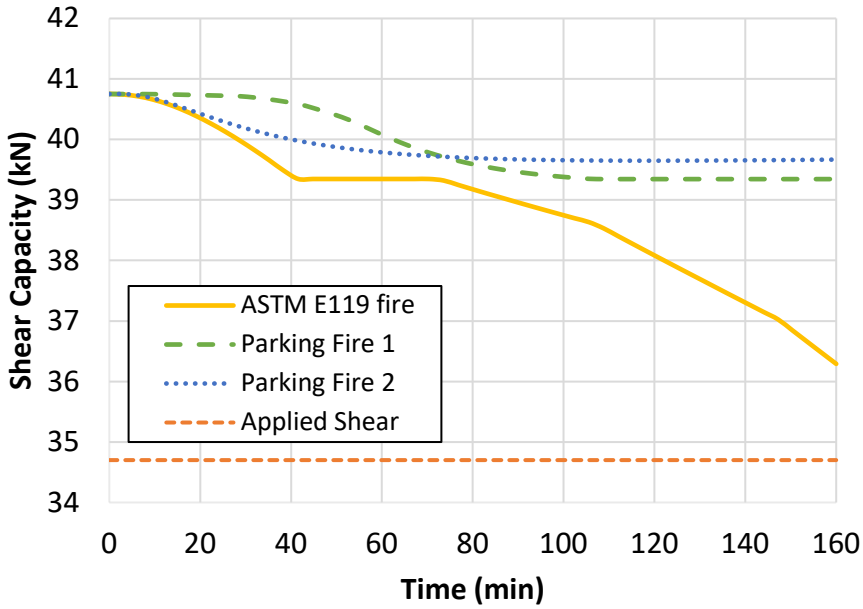

Figure 11 Comparison of degradation in shear capacity under standard and realistic fire scenario

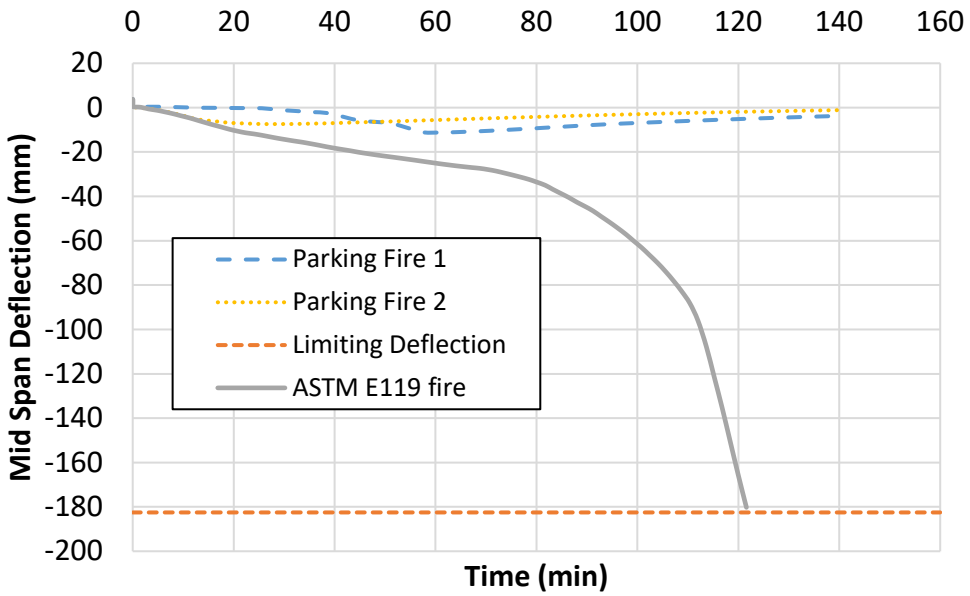

Figure 12 Comparison of mid-span deflections under standard and realistic fire scenario